IOP Conf. Series: Materials Science and Engineering **382** (2018) 022059 doi:10.1088/1757-899X/382/2/022059

Hydrothermal Synthesis of Mn-doped VO_2 (B) as Cathode Material for Lithium-ion Battery

HAN Shichang, ZOU Zhengguang[1], HUO Shuailei

College of Material Science and Engineering, Guilin University of Technology, Guang'xi, Guilin 541004, China

Email: zouzgglut@163.com

Abstract. Mn-doped VO_2(B) was synthesized via a hydrothermal reaction from manganese sulfate ($MnSO_4$) and Vanadyl oxalate ($VOC_2O_4{\cdot}5H_2O$). The effects of the content of Mn on the electrochemical performance of material were studied by means of galvanostatic charge-discharge, cyclic voltammetry and electrochemical impedance spectroscopy (EIS). Compared with pure material VO_2(B), the Mn_xVO_2(B) which was doped with little Mn(x=0.01,0.02,0.05) had higher specific capacity and more preferable cycle performance. When galvanostatic charged-discharged with 0. 1 C in 1.5-4.0 V. the initial discharge specific capacity of sample Mn_1, Mn_2 and Mn_3 were 204 mAh g^{-1}, 242 mAh g^{-1} and 249 mAh g^{-1} respectively larger than pure VO_2 sample (181mAh g^{-1}).In particular, the sample of Mn_1 exhibited best electrochemical performance. The initial discharge capacity maintained 164 mAh g^{-1} after 50 cycles. The retention rate of capacity was 80%.

1. Introduction

In recent years, new energy vehicles, communications, energy storage and other emerging fields have been rapidly developed, which greatly promoted the development of large capacity , high energy density Rechargeable lithium-ion batteries (LIBs)[1-3]. For the positive electrode active material for energy storage, improve energy density is to improve the discharge voltage and discharge capacity. At present, in order to improve the energy density as the main development goals of the third generation of lithium-ion batteries, the cathode material is at the stage of upgrading.

Vanadium oxides exist in various compositions(VO_2,V_2O_3,V_6O_{13},V_3O_7,V_2O_5,etc.) depending on the oxidation state (+2 to +5) of vanadium[4-11]. Among which, metastable VO_2(B) has a potential usage as a cathode materialsin LIB. Due to its open framework structure with edge-sharing VO_6 [4,5,11]octahedra which permitted the lithium ions rapidly intercalation/deintercalation between the layers,This special structure makes it possible to achieve a theoretical reversible capacity of 324 mAh g^{-1} .

However, due to inferior electronic conductivity and poor cycle stability of VO_2(B), it seriously affected its practical application. In recent years, in order to solve these problems effectively, the electrochemical properties of vanadium oxides have been improved by doping[12-14],cladding[15-17], nanocrystallization[18-23],and othermethods[24]. CHENG H, et al[12]synthesized Cu_xVO_2,with Cu^{2+} doping, the Fermi level of Li in VO_2(B) and the conductivity have promoted, the ability of the Lithium-ion insertion and extraction and the stabilityof the charging and discharging were improved as well. When the amount of doping Cu^{2+} is 1.03at%, the charge and discharge performance of VO_2(B) had improved at low and high rate, the discharge specific capacity for the first time is 317.1 mAh g^{-1} at 0.132C, along with after 51 cycles measurement, the specific capacity was still kept 234.3mAh g^{-1}.

In this article, we synthesized pure VO_2(B) and Mn-doped VO_2(B) through the hydrothermal reaction combining with the calcination process and investigated the structural and electrochemical characteristics of Mn_xVO_2(B) electrodes during cycling tests in lithium-ion batteries.

2. Numerical Investigation

2.1 Synthesis of Mn doping VO_2(B)

All chemical reagents were analytical grade and implemented without any further purification. Mn-doped VO_2 were ready according to the following procedure. 0.4g Vanadium pentoxide and 1.25g Oxalic acid dihydrate were dissolved in 20mL of deionized water. The mixed solution was kept under stirring at 70℃ in a water bath until a blue colored solution formed. And then naturally cooled to room-temperature.Then the obtained precursor solution filtration. The suitable amount of manganese sulfate was dissolved in 30mL of deionized water when it completely dissolves, pour it into as-synthesized Vanadyl oxalate solution, then 3ml 30%(H_2O_2) was added to the mixed solution, after stirring it without come up to bubbles and transferred into a 100mL Teflon-lined autoclave. The autoclave was sealed and maintained at 160℃ for 24 h and then cooled to room temperature naturally. The precipitate was washed three times with deionized water and alcohol, respectively and dried in the freeze dryer for 24 h. Finally, the obtained precursor was sintered at 350℃ at 3℃/min for 1 h in argon. Molar ratios of Mn to V were increased gradually from 0 to 1/20. The samples were identified as Mn_0, Mn_1, Mn_2 and Mn_3, corresponding to different molar ratios of Mn to V (0, 1/100, 1/50, 1/20).

2.2 Characterization

The X-ray powder diffractometer (XRD) with a Cu Kα radiation source (λ = 0.154 nm, the scanning rate of 6 °/min) was used to analyze the phase of the products. The Hitachi S-4800 field emission scanning electron microscopy (FESEM) was carried out to observe the morphology of the products.

2.3 Electrochemical measurements

The positive electrode was prepared by mixing active material, acetylene black carbon powder and polyvinylidene fluoride (PVDF) binder in a weight ratio of 7/2/1, grinding the mixture with a certain amount of N-methy1-2pyrrolidone (NMP), then the slurry was coated uniformly on Mn foil. The Mn foil was dried in vacuum at 90℃ for 12 h. 1 mol/L $LiPF_6$ in a mixture of dimethyl carbonate (DMC)，ethylene carbonate (EC) and diethyl carbonate (DEC) were used as an electrolyte (DMC/EC/ DEC=2:2:1 in volume). The cells were assembled in a glove box filled with pure dry argon gas. Galvanostatic charge/discharge measurements were carried out in the voltage region between 1.5 V and 4.0 V. Both the electrochemical impedance spectroscopy (EIS) and the cyclic voltammetry (CV) were tested through a CHI 760D electrochemical workstation, and the CV measurement was performed in the potential range from 4.0 to 1.5 V at a scan rate of 0.1 $mv.s^{-1}$

3. Results and discussion

Figure 1(a) showed the XRD patterns of Mn_xVO_2（x=0.00,0.01,0.02,0.05）synthesized at 350℃. All peaks were basically consistent with the standard diffraction peaks of VO_2(B) (JCPDS no. 81-2392). It became apparent that compounds are well-crystallized. As can be observed figure 1(b), with the doping content increasing, the diffraction peaks broaden and the intensity weakens, which was attributed to the crystallinity decrease after doping with Mn^{2+}.

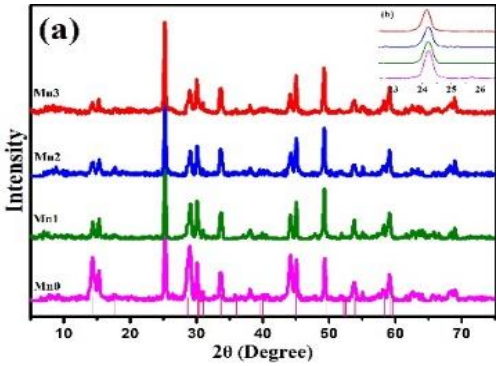

Figure 1 (a) XRD patterns of Mn_0(0.00), Mn_1(0.01), Mn_2(0.02), Mn_3(0.05)and (b) their high angle patterns at 2θ degrees ranging from 24° to 27°

3.1 Electrochemical measurements

Figure 2 showed the FESEM images of pure VO_2 and Mn-doped VO_2 samples fabricated of Mn_0(a), Mn_1(b), Mn_2(c) and Mn_3(d). In the figures, it can be easily seen that the structure units of pure VO_2 and Mn-doped were nanosheets. Meanwhile, we can see that the doping content of Mn^{2+} was significant effect on the morphologies of as-synthesized products. Due to the doping of manganese, the morphology of the product is formed from irregular flakes into flowerlike architectures. The shape of the product becomes finer and longer as the doping amount increases, which would further influence the electrochemical performance.The length of pure VO_2 nanosheets was about 500-1000nm and the length of $Mn_{0.05}VO_2$(B) was about 3000-4000nm.

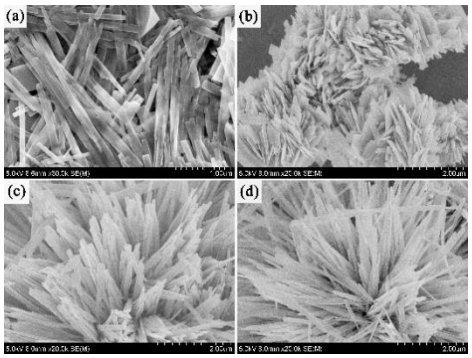

Figure 2 FESEM images of Mn0(a, b), Mn1(c, d), Mn2(e, f) and Mn3(g, h)

3.2 Electrochemical properties

Figure 3a displayed the cycling performance of Mn-doped samples. The charge and discharge curves at the current density of 32.4 mAh g^{-1} in 1.5−4.0 V. it can be seen from Figure 3a that all doping samples VO_2 discharge performance were better than pure VO_2. The initial and after 50 cycles discharge capacities were 181 mAh g^{-1} and 124 mAh g^{-1} (Mn_0), 204 mAh g^{-1} and 164 mAh g^{-1} (Mn_1), 242 mAh g^{-1} and132mAh g^{-1} (Mn_2), 249 mAh g^{-1} and 129 mAh g^{-1} (Mn_3). The retention rates of capacities were 69%, 80%, 55%, and 51.8%, respectively. Obviously, the first discharge specific capacity increases with the increase of Mn doping. However, the cycle performance did not augment with the increase in manganese doping. Among which, Mn1 showed the best cycling performance of 80% after 50 cycles at 0.1C. The result suggested that doping appropriate Mn^{2+} could stabilize the crystal structure of VO_2(B) and reduce the irreversible destruction of cathode materials. Combined with scanned images, we see that the addition of manganese make better dispersion of samples, simultaneously the sample becomes more subtle. It can be drawn from the structure of the sample that slender flower samples are not conducive to the stability of the battery.

Figure 3 (b) to (c) showed the 1th charge-discharge curves of different doping content of the

samples at the current density of 32.4 mA g^{-1} in the voltage ranging from 1.5 V to 4.0 V at room temperature. All of them showed a distinct charge platform at around 2.7 V and a distinct discharge platform at around 2.5V , the result was agreement with that of the reference [25, 26].

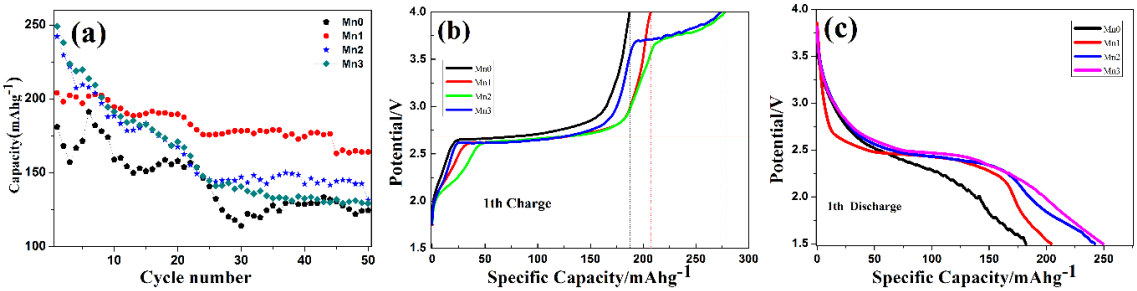

Figure 3 a Cycling performance of the pure VO2(Mn0) and Mn -doped VO2(Mn1, Mn2, Mn3) electrodes at 0.1 C； b-c Charge–discharge profiles at 0.1C between 1.5 and 4.0V

3.3 Electrochemical properties

Figure 4 showed the Nyquist plots of the samples, the Nyquist plots were measured by EIS(electrochemical impedance spectra) after cycling for 2 times, It can be seen from figure 4 that the charge transfer impedance (Rct) value of Mn_0, Mn_1, Mn_2 and Mn_3 in the high-frequency region's semicircles were corresponding to 1184Ω, 1430 Ω， 1980 Ω and 1060 Ω respectively. Obviously, the charge transfer impedance of Mn_1, Mn_2 is larger than Mn_0. Attributed to because the flake structure of samples became finer long after doping,consequently the contact area between the sheet and the sheet is diminutive. Therefore, the lithium ion has a longer diffusion distance between the particles, thereby the charge transfer resistance between the electrode and electrolyte aggrandized significantly. Meanwhile, Rct value of Mn_3 was found to be the smallest, which indicates that the addition of more manganese ions to replace the vanadium position, will make the structure conducive to the transmission of lithium ions.

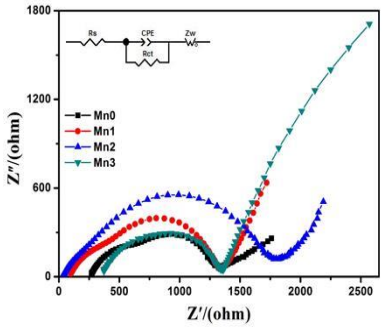

Figure 4 the Nyquist plots of the samples with different stirring rates

Figure 5 showed the cyclic voltammetry curves of Mn_0, Mn_1, Mn_2 and Mn_3 with the voltage range of 1.5-4.0 V in the scanning speed of 0.2 mV/s after cycling for 2 times. A pair of oxidation and reduction peaks could be observed in the figure, which represents the extraction and **insertion** of Li^+ during the electrochemical processes. The peak shape of the sample has good symmetry, indicating that the electrochemical performance before and after doping is relatively stable. With the increase of manganese content, the oxidation peak shifts to low potential and then the high potential, whilst the reduction peak shifts to the high potential and then to the low potential, which indicates that doping can affect the polarization of the material. In addition, the area of the curve in the sample of Mn_3 was the biggest, which represented the sample capacity of Mn_3 was the largest.

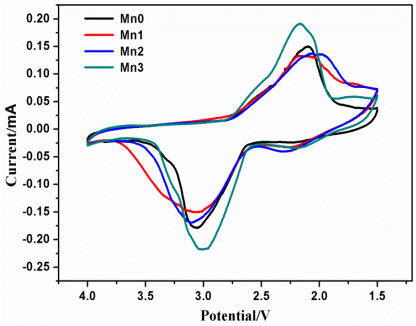

Figure 5 Cyclic voltammetry (CV) curves of Mn0, Mn1, Mn2 and Mn3.

4. Conclusion

Pure VO_2(B) and Mn-doped VO_2(B) were synthesized via a completely aqueous solution based synthesis method from manganese sulfate ($MnSO_4$) and Vanadyl oxalate ($VOC_2O_4 \cdot 5H_2O$). It was noted that the incorporation of Mn^{2+} significantly affected the morphology and structure of VO_2(B). With the increase of manganese content, the nanobelts became thin and long, the morphology changed from irregular state to flower-like structures. Electrochemical properties demonstrated that the charge/discharge capacity of the samples have been enhanced greatly after doping with Mn^{2+}. In particular, the sample of Mn_1 exhibited the best electrochemical performance. The initial discharge capacity was 204mAh g^{-1} and maintained 164mAh g^{-1} after 50 cycles. The retention rate of capacity was 80%. Far more than samples of Mn_0, $Mn_2$and Mn_3.

Acknowledgements

Supported by the National Natural Science Foundation of China (51562006).

References

[1] Armand M, Tarascon J M. Building better batteries[J]. Nature, 2008 , 451(7179):652-657.
[2] Li H. Fundamental scientific aspects of lithium batteries——Summary and outlook. Energy Storage Science and Technology [J], 2015, 4(3):306-318.
[3] Luo F，Liu B ， Zheng J ， et al. Review-Nano-silicon/carbon composite anode materials towards practical application for next generation Li-ion batteries[J].Journal of the Electrochemical Soci ety, 2015, 162(14):2509-2528.
[4] Wu, C. & Xie, Y. Promising vanadium oxide and hydroxide nanostructures: from energy storage to energy saving. Energy Environ.Sci. 1010(3): 1191–1206.
[5] Liu H, Wang Y, Wang K, Hosono E , et al. Design and synthesis of a novel nano horn VO_2(B) hollow microsphere and theirapplication in lithium-ion batteries[J]. J. Mater. Chem. 19, 2835–2840 (2009).
[6] Li H, He P, Wang Y, Hosono, E, et al. High-surface vanadium oxides with large capacities for lithium-ion batteries: from hydrated aerogel to nanocrystalline VO_2(B), V_6O_{13} and V_2O_5[J]. J. Mater. Chem. 2011,21:10999–11009.
[7] Murphy D W, Christian P A, Solid state electrodes for high energy batteries[J]. Sci, 1979, 205(4407):651.
[8] Glanz J. Lithium battery takes to water - and maybe the road[J], Sci,1994,264(5162):1084.
[9] Natasha A, Megan R, Anne C. Dillon, M. Layered Vanadium and Molybdenum Oxides: Batteries and Electrochromics[J]. J. Mater.Chem, 2009,19(17):2526-2552.
[10] Emmanuel B, Guillaume S, Dominique L, et al. Preparation of Nanotextured VO2[B] from Vanadium Oxide Aerogels[J].Chem Mater, 2006(18)18:4369-4374.
[11] Armstrong G, Canales J, Armstrong, et al. The synthesis and lithium intercalation electrochemistry of VO_2(B) ultra-thin nanowires. J. Power Sources 178,723–728 (2008).
[12] CHENG H. Study on Synthesis, Doping and Property of Vandium Oxide as Cathode Materials[D]. Guangxi: Guilin University of Technology, 2014.

[13] Zhan S Y. Synthesis and electrochemical properties of metal doped V2O5 Cathode material for Li-ion batteries[D]. Jilin: Jilin University, 2010.
[14] Yan Z Y, Zou Z G, Long F, et al. Synthesis and Electrochemical Properfties of Cr Doped V6O13 Cathode Materials for Li -ion Batteries[J]. JOURANAL OF SYNTHETIC CRYSTALS, 2015, 44(8): 1-8.
[15] Zhao Q Q, Jiao L F, Peng W X, et al. Facile synthesis of VO2(B)/carbon nanobelts with high capacity and good cyclability[J]. J. Power Sources, 2012, 199: 350-354.
[16] Reddy C, Rambabu B, Kusum K ,et al. VO_2(B) @ carbon cathodes for lithium ion batteries Colloids and Surfaces A: Physicochem. Eng. Aspects, 481 (2015) 314–318.
[17] Li W Y, Zhang Z Y, Tang Y B, et al. Graphene-Nanowall-Decorated Carbon Felt with Excellent Electrochemical Activity Toward VO^{2+} /VO^{2+} Couple for All Vanadium Redox Flow Battery[J]. Advanced science,2016,3:2-7.
[18] Liu P, Zhu K, Gao Y,et al. Ultra-long VO_2 (A) nanorods using the high-temperature mixing method under hydrothermal conditions: synthesis, evolution and thermochromic properties[J]. Crystengcomm, 2013, 15(14):2753-2760
[19] Reddy C V S, Walker E H, Wicker S. A, et al. Synthesis of VO_2(B) nanorods for Li battery application[J]. Curr. Appl. Phys., 2009, 9:1195.
[20] Li G C, Pang S P, Jiang L, et al. Environmentally friendly chemical route to vanadium oxide single- crystalline nanobelts as a cathode material for lithium-ion batteries[J]. Phys. Chem. B, 2006, 110(19) :9383.
[21] Niederberger M, Muhr H J, Krumeich F, et al. Low-Cost Synthesis of Vanadium Oxide Nanotubes via Two Novel Non-Alkoxide Routes[J]. Chem. Mater., 2000, 12(7):1995-2000.
[22] Krumeich F, Muhr H J, Niederberger M, et al. Morphology and Topochemical Reactions of Novel Vanadium Oxide Nanotubes[J]. Cheminform, 1999, 30 (51): 8324.
[23] Chen X Y, Wang X, Zhang H, et al. An ethylene glycol reduction approach to metastable VO_2 nanowire arrays[J]. Nanotechnology, 2004, 15(11):1685.
[24] Andrukaitis E, Ian Hill. Diffusion of lithium in electrodeposited vanadium oxides[J]. Power Sources, 2004,136(2):290-295.
[25] Chen Z J, Gao S K, Jiang L L, et al. Crystalline VO(B) nanorods with a rectangular cross-section[J]. Mater. Chem. Phys., 2010, 121(1-2):254-258.
[26] Reddy C V S, Walker E H, Wicker S A, et al. Synthesis of VO(B) nanorods for Li battery application[J]. Appl. Phys., 2009, 9:1195.